Solar Energy Materials & Solar Cells 266 (2024) 112645

Contents lists available at ScienceDirect

Solar Energy Materials and Solar Cells

journal homepage: www.elsevier.com/locate/solmat

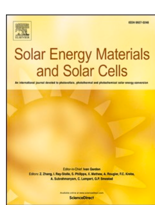

Stability of industrial gallium-doped Czochralski silicon PERC cells and wafers

T. Niewelt [a,b,c,*], F. Maischner [b,c], W. Kwapil [b,c], E. Khorani [a], S.L. Pain [a], Y. Jung [d], E.C.B. Hopkins [a], M. Frosch [c], P.P. Altermatt [e], H. Guo [f], Y.C. Wang [f], N.E. Grant [a], J.D. Murphy [a]

[a] School of Engineering, University of Warwick, Coventry, CV4 7AL, United Kingdom
[b] Fraunhofer Institute for Solar Energy Systems ISE, Heidenhofstraße 2, 79110, Freiburg, Germany
[c] Chair for Photovoltaic Energy Conversion, Department of Sustainable Systems Engineering (INATECH), University of Freiburg, Emmy-Noether-Str. 2, 79110, Freiburg, Germany
[d] Institute for Energy Technology, Korea University, 02841, Seoul, Republic of Korea
[e] Trina Solar Limited, State Key Laboratory for PV Science and Technology (SKL), Changzhou, 213031, China
[f] Silicon Wafer Business Unit, LONGi Green Energy Technology Co. Ltd., Xi'an, 710100, China

A B S T R A C T

The carrier lifetime stability of gallium-doped silicon wafers and performance stability of industrial PERC solar cells produced from sister wafers were investigated under four different illumination conditions and temperatures. The seven investigated materials feature a resistivity variation of 0.4–1.0 Ωcm and lifetime samples were processed to create high hydrogen content (with PECVD SiN_x) or low hydrogen content (with ALD Al_2O_3 or HfO_2). Our results confirm that the material itself *is* prone to light and elevated temperature induced degradation (LeTID), however experiments on PERC cells produced utilising the same silicon material indicate that the production process can successfully suppress LeTID. In contrast to earlier studies, we observe only small levels of degradation at the cell level, with some showing an improvement in cell parameters under LeTID testing conditions. Our results indicate that LeTID is not necessarily a major issue for the performance of modern passivated emitter and rear cells made from gallium-doped silicon substrates.

1. Introduction

The degradation of solar cells upon exposure to illumination at elevated temperatures – that is during field operation conditions – addressed as light and elevated temperature induced degradation (LeTID) has been a major source of uncertainty for the stability of passivated emitter and rear cell (PERC) devices. The effect was first reported as a degradation effect of PERC cells made from boron-doped multicrystalline silicon in 2012 [1] but was later found in other materials and identified to arise from activation of a bulk defect, e.g., Refs. [2–7]. Efficiency degradation around $5\%_{rel}$ and up to $10\%_{rel}$ has been reported [3,8] and the effect has been linked to excess bulk hydrogenation [2–4,7,9–11].

The photovoltaic industry has recently undergone a substantial change in substrate doping, when the prevalent dopant for *p*-type doping changed from boron to gallium. The less favourable segregation coefficient of gallium compared to boron complicates growing crystals with a tight resistivity range [12,13]. In return, the absence of boron in Czochralski-grown (Cz-Si) silicon relaxes the constraints for oxygen incorporation by avoiding the formation of Boron–Oxygen Defects and hence light-induced degradation (LID) [14,15]. Another central motivation for the shift to gallium doping was indications that this material could be robust to LeTID. This suggestion has been questioned and there are studies demonstrating characteristic degradation effects in gallium-doped silicon, e.g., Refs. [16–18]. Several studies on the basis of charge carrier lifetime test structures have reported degradation when Cz-Si:Ga samples were subjected to LeTID testing, e.g., Refs. [7,18–21]. Investigations of cell precursors or finished solar cells made from Cz-Si:Ga substrates have reported both good stability [22–24] or significant degradation [25,26]. The performance degradation due to LID and LeTID have many similarities in overall behaviour, and both are known to recover upon extended exposure. In this direct comparison, a mismanaged LeTID will likely have a worse effect on module energy production yield due to the slower recovery timescale – LeTID can be expected to affect most of the module lifespan [8]. Most studies on the topic of LeTID in Ga-doped silicon have investigated specific aspects such as one specific sample type and a narrow window of stability testing conditions. In this study, we perform a wide variety of stability tests on typical industrial Ga-doped Cz-Si wafers and industrial PERC cells produced on the same material. This serves to demonstrate that the

* Corresponding author. School of Engineering, University of Warwick, Coventry, CV4 7AL, United Kingdom.
E-mail address: tim.niewelt@ise.fraunhofer.de (T. Niewelt).

https://doi.org/10.1016/j.solmat.2023.112645
Received 14 July 2023; Received in revised form 17 October 2023; Accepted 14 November 2023
0927-0248/© 2023 The Authors. Published by Elsevier B.V. This is an open access article under the CC BY license (http://creativecommons.org/licenses/by/4.0/).

robustness to LeTID of modern PERC cells originates in large part from adaptions within the cell process, as the material itself is still prone to degradation.

2. Experiments

2.1. Samples

A series of experiments was performed on a set of Cz-Si:Ga wafers from a major industrial supplier. Several boron-doped reference wafers were also used. The gallium-doped sample set consists of seven groups A-G that span a resistivity range of ~0.4–1.0 Ωcm. This resistivity range covers industrial production of PERC and similar solar cell concepts. The sample groups are listed in Table 1 with the information provided by the manufacturer. From each group, half of the wafers were processed into PERC cells by Trina Solar in an old industrial production line. The cell efficiencies as processed were in a range 22.4–22.8 % and within the typical range of the used facility at the time (i.e., 2020). We did not observe systematic differences in efficiency between the materials used.

The second half of wafers were processed to symmetrically passivated *lifetime samples* to assess the potential impact of LeTID on material quality. We based this sample set on the known impact of high hydrogen containing dielectrics during solar cell production on the formation of LeTID. The silicon wafers from all material groups listed in Table 1 were subjected to phosphorus diffusion gettering (emitter resistance ~83 Ω/□) followed by fully etching back the diffused region, resulting in final sample thicknesses around 150 µm for all lifetime samples. The samples were subsequently coated with 75 nm of SiN_x (refractive index $n_{nitride}$ = 2.015) by a plasma-enhanced chemical vapour deposition (PECVD) process. Following the SiN_x deposition, the samples were then fired in an industrial furnace, whereby the process was tuned to achieve a peak sample temperature of 800 °C and an average cooling rate of 81 K/s (whilst above a temperature of 600 °C) as outlined by Maischner et al. [27]. The SiN_x layers and the firing processes used in this study were based on an experiment by Maischner et al. whom demonstrated that such conditions produce a significant LeTID effect in materials they investigated [28]. The samples for this study were processed alongside the samples discussed in Ref. [28]. Boron-doped Cz-Si and FZ-Si wafers were included in the experiments for comparison (see Table 1).

Table 1
Studied material groups. Groups A-G are Cz-Si:Ga wafers. The resistivity range of the wafers and a representative interstitial oxygen concentration [O_i] were provided by the supplier.

Material	Resistivity [Ωcm]	[O_i] [ppma]
A ■ (red)	1.03–0.85	14
B ■ (orange)	0.85–0.77	8.1
C ■ (yellow)	0.77–0.70	7.8
D ■ (green)	0.7–0.64	8.9
E ■ (blue)	0.64–0.54	9
F ■ (dark blue)	0.54–0.46	9.5
G ■ (purple)	0.46–0.37	9.3
Cz:B ⊠	~0.8	unknown
FZ:B □	2.4	unknown

Based on literature, the main impact on LeTID is suspected to be the degree of bulk material hydrogenation. We also created a second type of samples with low bulk hydrogenation from the same Cz-Si:Ga materials. The samples and their testing are discussed in the Appendix.

2.2. Experiments

Various experiments were performed to assess the impact of LeTID at a material and cell level under different conditions. These experiments are numbered and listed in Table 2. **Experiments I-III** were performed on the lifetime samples cleaved from processed wafers to investigate whether the gallium-doped material itself is susceptible to LeTID and whether there is an impact of doping concentration. Degradation was assessed in terms of changes of charge carrier lifetime, which were monitored with photoconductance decay (PCD) measurements using Sinton WCT-120 lifetime testers (software version 5.73.2). In addition to effective charge carrier lifetime measurements, we tracked the variation of measured sample sheet resistance and the surface recombination parameter J_{0s}. The sheet resistance (measured by the WCT-120 directly before flashing) can reveal pronounced changes in sample doping that may arise, e.g., due to formation or dissolution of dopant-hydrogen pairs, as discussed and studied, e.g., by Walter et al. [29] and Hammann et al. [30]. Monitoring J_{0s} during stability experiments is useful to distinguish between the activation of defects in the wafer bulk and close to its surfaces [31,32]. This is especially useful since the sample processing and stability testing conditions of LeTID studies are known to give rise to degradation of surface passivation quality, as demonstrated, e.g., by Sperber et al. [33].

The first experiment, **Experiment I,** was LeTID testing performed on lifetime samples by subjecting them to an illumination intensity of 0.15 sun equivalents at 75 °C. The rather low intensity when compared to the common 1 sun eq. intensity was chosen deliberately based on reports that this may give rise to more pronounced LeTID in Cz-Si:Ga [18]. Also, application of a lower excess carrier generation rate on lifetime samples can be useful since the arising excess carrier density is more comparable with the conditions that would be observed in finished solar cells during LeTID testing (where diffused regions and metal contacts give rise to additional recombination). The same conditions were also applied to samples with a different passivation scheme with low bulk hydrogenation, as discussed in the appendix.

For **Experiment II**, lifetime samples were subjected to an accelerated LeTID test by illumination with 2 sun eq. illumination at 140 °C. According to Maischner et al. [28,34] these conditions allow for accelerated testing of LeTID stability on both wafer and solar cell level. Elevated temperature in the dark has been demonstrated to activate LeTID defects in boron-doped silicon, e.g., by Chen et al. [35]. To investigate whether this effect can also be observed in Cz-Si:Ga material, lifetime samples were subjected to dark annealing at 175 °C in **Experiment III**.

Potential LeTID of the finished PERC cells was investigated in **Experiments IV-IX** by exposing them to unbiased LeTID testing (i.e., in V_{oc} condition). The chosen conditions resemble the conditions described above. Most experiments were performed on the basis of the PL proxy method introduced by Grant et al. in Ref. [16]. This method applies steady state PL imaging of fixed illumination intensity and integration time and evaluates the count rate caused by luminescent recombination. This signal is a direct probe of charge carrier density under open circuit conditions – and hence relates to charge carrier lifetime. Due to the quadratic relation between carrier density and luminescence intensity on one hand and the logarithmic relation to device voltage on the other hand, this method allows detection of small changes within the solar cell that may be difficult to track in classical IV parameter testing.[1] In **Experiment IV**, tokens cleaved from the solar cells were subjected to 1

[1] See the appendix for the relation between PL intensity changes and device voltage.

Table 2
Overview of the different experiments performed in this study.

Experiment	Sample type	# of tested Cz-Si:Ga materials	Temperature (°C)	Intensity (sun eq.)	Characterisation
I	PECVD lifetime, *highH*, 5 × 5 cm^2	3	75 ± 3	0.15 ± 0.05	PCD
II	PECVD lifetime, *highH*, 5 × 5 cm^2	4	140 ± 3	2 ± 0.3	PCD
III	PECVD lifetime, *highH*, ~5 × 6 cm^2	4	175 ± 5	0	PCD
IV	Cell tokens, 5 × 5 cm^2	7	75 ± 5	1 ± 0.15	PL proxy
V	Cell tokens, 5 × 5 cm^2	7	75 ± 5	0.15 ± 0.08	PL proxy
VI	Full cell	1	140 ± 3	2 ± 0.3	PL proxy
VIIa	Cell tokens, 5 × 5 cm^2	6	175 ± 5	0	PL proxy
VIIb	Full cell	1			
VIII	Full cells	6	175 ± 5	0	IV (LOANA)
IX	Full cells	2	300 ± 5	0	IV (LOANA)

sun eq. illumination at 75 °C. Following the observation of Kwapil et al. [18] that LeTID may be more pronounced in Ga-doped material when subjected to low injection conditions, we also applied a low intensity of 0.1–0.15 sun eq. illumination at 75 °C to cells and monitored their progression over time (**Experiment V**). Low intensity illumination at V_{oc} is also somewhat more reflective of field conditions, since during *maximum power point* operation the majority of excess carriers would be extracted. An additional test was performed under accelerated LeTID testing conditions of 2 sun eq. at 140 °C on one cell (**Experiment VI**). The impact of dark annealing at 175 °C on PERC cells was studied in detail by comparing the PL proxy method (**Experiment VIIa** & **b**) to the results of full dark and light IV curve measurements in a LOANA tool (**Experiment VIII**). In view of findings in previous work by Grant et al. that the stability of Ga-doped PERC cells during degradation tests might change significantly when subjected to a 30 min 300 °C dark anneal [16, 17], all experiments on solar cells featured samples both as-manufactured and after such a pre-anneal. While such treatments are not typical in cell or module production, it serves to test the effect of a redistribution of hydrogen across the cell which may occur during a module's lifetime. The direct impact of such an anneal at 300 °C on solar cell IV parameters was monitored in **Experiment IX**.

Different setups were used to realise the vastly different experimental conditions. All experiments were conducted on laboratory hotplates and the temperatures given in Table 2 are set temperatures along with uncertainty estimates based on the laboratory conditions. For dark annealing, samples were either packed between two sheets of aluminium foil and a pre-warmed metal weight placed on top (**Experiments III** & **VII**) or hotplates with a lid were used, ensuring a hot air environment (**Experiments VIII** & **IX**). Illumination was either realised with halogen lamps (**Experiments II**, **IV** & **V**) with the intensity determined by a Amprobe Solar-100 light meter or with white light LED arrays (**Experiments I** & **VI**) where the intensity was measured *via* the current of a pre-characterised solar cell (c.f., [36]). The given uncertainty ranges reflect the spatial intensity variation found for the setups and the impact of lamp degradation during long experiments.

3. Results

3.1. Material/lifetime samples

As discussed in section 2, **Experiments I-III** studied the charge carrier lifetime reaction of simple test structures (lifetime samples) to different LeTID testing conditions. All lifetimes reported here were extracted at an excess carrier density Δn of 10^{15} cm^{-3}. Given the doping density N_{dop} varies between the different materials, this means different injection conditions were achieved. We ensured that this choice of a fixed excess carrier density used for lifetime evaluations did not affect the reported trends. This was done *via* comparison with measurements extracted at a constant $\Delta n/N_{dop}$ ratio and at the respective cross-over point of FeGa pairs and interstitial iron, which was calculated with the parameters reported by Post et al. [37].

3.1.1. Moderate LeTID testing

Our pretests on lowly hydrogenated samples demonstrated good initial material quality of the investigated Cz-Si:Ga wafers (as discussed in the appendix). For LeTID testing, a moderate temperature of 75 °C and a low intensity illumination were chosen to mimic the conditions of module operation. The experiment spans more than 1000 h of total testing. Fig. 1a) demonstrates that under moderate testing conditions of **Experiment II**, the Cz-Si:Ga samples show a slight degradation in lifetime around 100 h of treatment time, which is more noticeable for samples of higher lifetime (c.f., Materials B & F compared to Material G, which only degraded by a few μs). The FZ-Si:B reference samples (which were processed and treated alongside the Cz-Si:Ga samples) exhibit a typical LeTID degradation-regeneration cycle within the first ~40 h of testing followed by a second degradation due to an increase in surface recombination (c.f,. Fig. 1c)). The Cz-Si:B samples show a pronounced improvement after 100 h of treatment time likely driven by regeneration of BO-defects [15]. We do not observe pronounced features in the fitted J_{0s} of Cz-Si samples beyond small fluctuations that should be expected when overall effective lifetime of the sample changes significantly (c.f., discussion in Ref. [32]). On the FZ-Si reference sample we observe a significant increase in fitted J_{0s}, which is similar to the behaviour of surface related degradation (SRD) reported by Sperber et al. [10] who however applied more intense illumination.

3.1.2. Accelerated LeTID testing

To verify the existence of LeTID in a given sample, it can be convenient to perform accelerated testing under more extreme conditions than would occur under operation. In this work, the *highH* lifetime samples were exposed to intense illumination (2 sun eq.) at elevated temperature (140 °C) in **Experiment III**. The carrier lifetime of the Cz-Si:Ga samples was found to degrade rapidly under these conditions, reaching its maximum degradation point in 1–2 min, after which the carrier lifetime recovered, as shown in Fig. 1b). We attribute this degradation regeneration cycle to LeTID. Interestingly, the lifetime decrease of FZ-Si:B reference samples appears to be caused only by SRD under these experimental conditions. Based on previous experiments on boron-doped material under these conditions, we consider it likely that the FZ-Si:B samples underwent the complete degradation regeneration cycle prior to the first data point being measured. In contrast, the behaviour of the Cz-Si:B sample is likely dominated by the deactivation of BO-defects [15] and the increase in fitted J_{0s} is likely not meaningful.

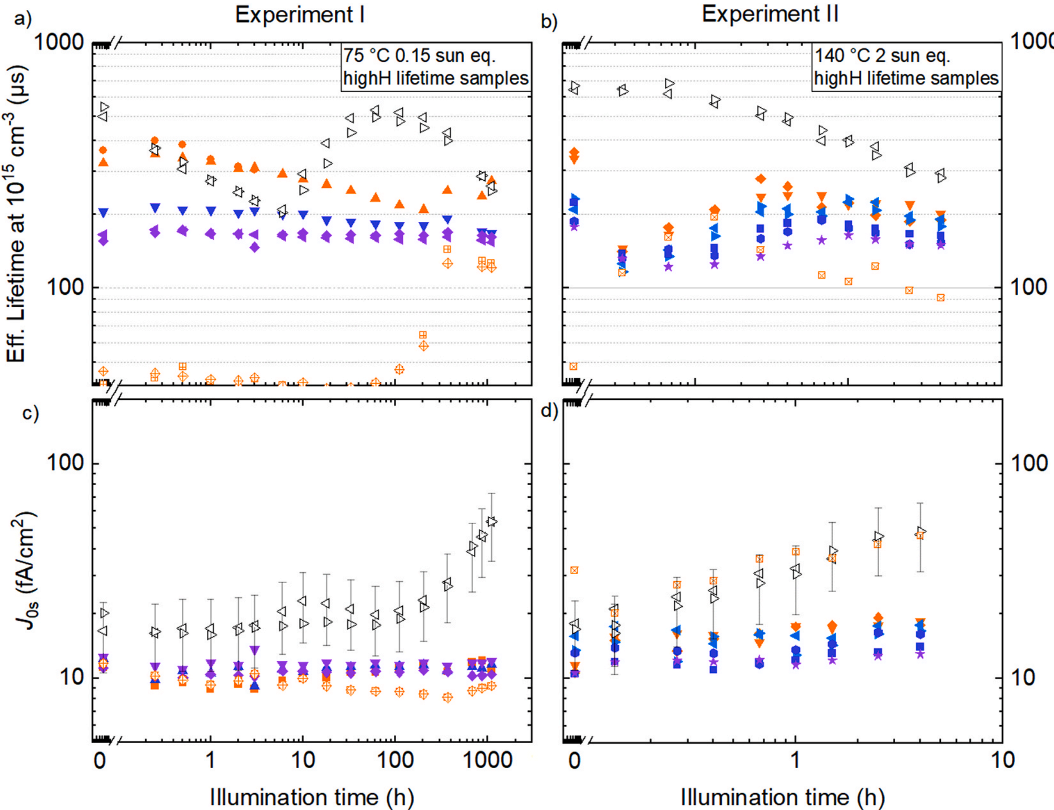

Fig. 1. Measurement results of LeTID testing on *highH* samples (fired with SiN_x passivation), i.e., **Experiments I & II**. a) & b): Effective charge carrier lifetimes τ_{eff} extracted at $\Delta n = 10^{15}$ cm^{-3}. c) & d): Fitted surface recombination parameter J_{0s} (shown error bars are representative for the expected uncertainty across the experiment). e) & f): Measured dark sheet resistance.

3.1.3. Dark annealing

Extended annealing in the dark allows the redistribution of hydrogen across the sample and between different configurations and complexes. In boron-doped silicon this has been shown to include the formation of the defect responsible for LeTID e.g. by Chen et al. [35]. The effect of dark annealing the hydrogenated Cz-Si:Ga lifetime samples at 175 °C (**Experiment III**) is shown in Fig. 2. We observed stable effective lifetime and no changes in surface passivation for tens of hours. This was followed by a decline in effective lifetime that was mirrored by an increase in the fitted J_{0s}, as shown in Fig. 2a) and b). Interestingly, this decline in effective lifetime is preceded by a markable decline in sheet resistance that appears to start around 5–10 h of treatment time, as shown in Fig. 2c). The observed resistivity changes are rather small compared to measurement uncertainties of the Sinton WCT-120 lifetime tester and therefore may be caused e.g., by the impact of temperature fluctuations. However, such effects occur less systematically, as illustrated by the respective resistivity traces for the other experiments on lifetime samples shown in Appendix Fig. 2. The systematic resistivity decrease implies the dissolution of GaH pairs, which appears to be about an order of magnitude slower compared to the work of Simon et al. who however annealed their samples at 180 °C [38]. **Experiment III** was very similar to the study presented by Kwapil et al. [18]. The main differences are our study featuring an Al_2O_3 layer between Cz-Si:Ga and SiN_x and the assignment of observed lifetime degradation to bulk or surface degradation. Thus we sourced the dark annealed sample from the study of Kwapil et al. [18] and tried to clarify the origin of degradation alongside three samples from **Experiment III**: the passivation layers were etched back and the samples were passivated using a low temperature temporary surface passivation scheme suggested by Grant et al. [39] (see Ref. [40] for the specific process used). The lifetimes measured with this temporary passivation were similar to before re-passivation and hence indicate that the degradation is not necessarily related to passivation quality.

3.2. PERC cells

As outlined in section 2, we performed LeTID stability testing under various conditions. Cells were heated to 75 °C and subjected to standard LeTID testing at either 1 or 0.15 sun eq. illumination intensity (**Experiment IV** and **Experiment V**, respectively) and monitored with the PL proxy method. The results are shown in Fig. 3a) and b). Where earlier studies of earlier Cz-Si:Ga PERC generations by Grant et al. [16,17] reported significant drops in PL intensity of up to 20 % - an indicator of LeTID defect activation - we found only small changes (~5 %) in our tests. The same was true for a full cell tested under the more extreme accelerated test conditions (140 °C and 2 sun eq.) in **Experiment VI** (see Fig. 3c)). Such small changes in PL translate to negligible change in cell voltage of less than 2 mV, which is below typical measurement uncertainties for solar cell IV testing.

Upon dark annealing at 175 °C, cells improved. When 5 × 5 cm^2 cell tokens were annealed in the dark in **Experiment VIIa**, the PL intensity increased by ~30 % within 10–100 h, as shown in Fig. 4a). Such intensity changes would imply a voltage increase of ~4–7 mV, which should be large enough to trace in IV curve measurements. However, the IV curves measured during dark annealing (**Experiment VIII**) did not reveal the same systematic behaviour, although small improvements of V_{oc} were observed, as shown in Fig. 4b)). The contacting unit of the LOANA tool used was not optimized for the metal grid layout at hand

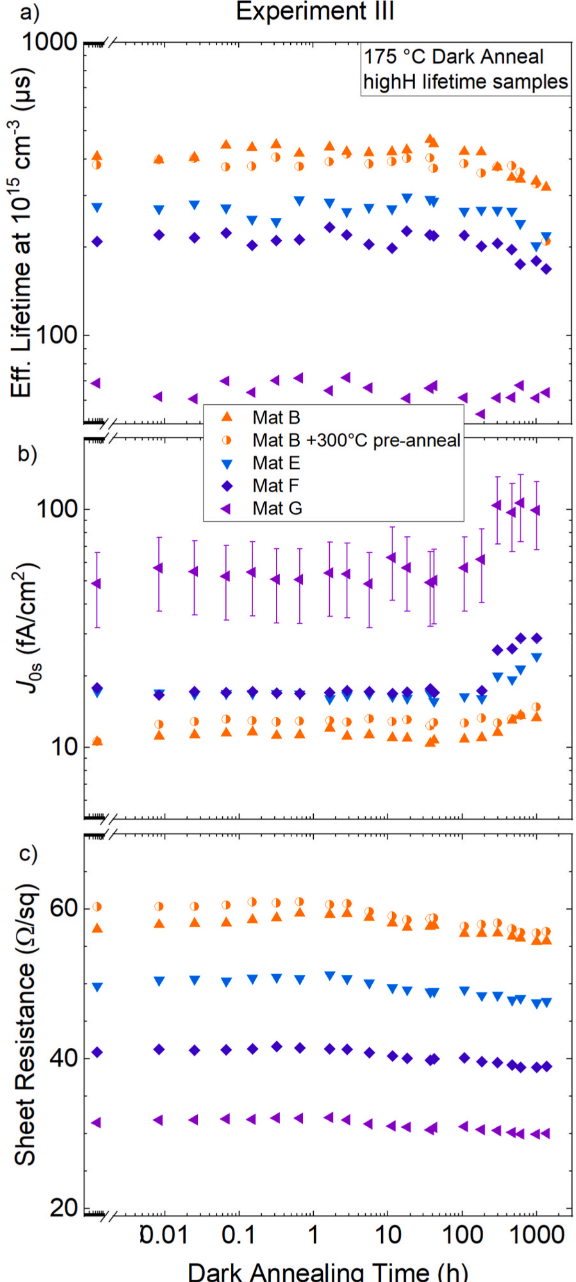

Fig. 2. Measurement results of dark annealing at 175 °C of hydrogenated Cz-Si:Ga lifetime samples, i.e., **Experiment III**. a) Effective charge carrier lifetimes τ_{eff} extracted at $\Delta n = 10^{15}$ cm^{-3}. b) Fitted surface recombination parameter J_{0s} (shown error bars are representative for the expected uncertainty across the experiment). c) Measured dark sheet resistance (see Appendix Fig. 2 for comparison).

and hence reproducibility of the cell contacting across the annealing time series was not ideal. This had a minor impact on the voltage measurement but significantly reduced reliability of current measurements and hence IV curve analysis. Keeping this in mind, automated fitting of the measured IV curves of the cell indicated a potential slight decrease of the cells' dark saturation current J_0 and an increase of the shunt resistance R_{shunt} with annealing time. These changes however did not translate into significant cell efficiency improvement. The mismatch between the expected and observed extent of voltage change in **Experiments VIIa** and **VIII** can possibly be attributed to sample size/type. The significant increase in PL intensity of the small sample tokens may be related to reduced edge recombination caused by oxidation of the

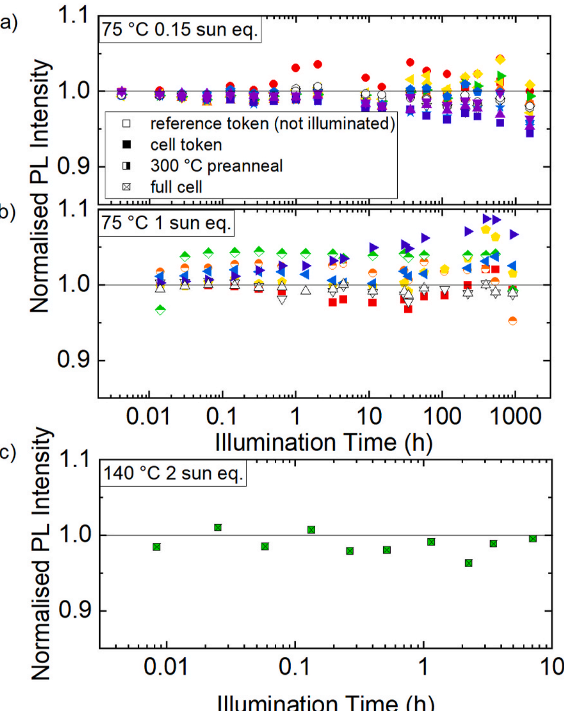

Fig. 3. LeTID testing of Ga-doped PERC solar cells monitored by the PL proxy method. The symbol colours are defined in Table 1. a) **Experiment V:** low intensity LeTID test (0.15 sun eq. at 75 °C) creating injection conditions lower than typical J_{mpp}; no systematic degradation or improvement observed throughout the experiment. Intensity changes <10 % across >1000 h of testing. b) **Experiment IV**: Standard LeTID testing conditions (1 sun eq. at 75 °C); no systematic degradation or improvement observed throughout the experiment. Intensity changes <10 % across >1000 h of testing. c) **Experiment VI**: Accelerated LeTID test (2 sun eq. at 140 °C [28]); no systematic PL intensity change observed throughout the experiment. Intensity changes less <5 % across 8 h of testing.

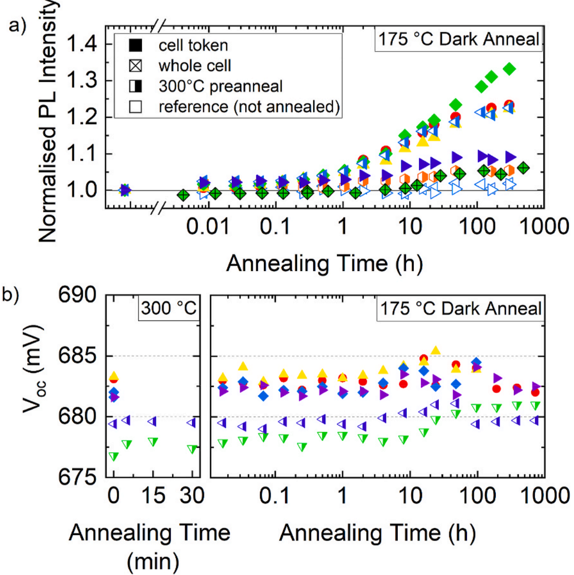

Fig. 4. a) **Experiment VII**: Dark Annealing of PERC cells at 175 °C monitored by the PL proxy method; a systematic improvement over time by up to 35 % is observed. b) **Experiments VIII** and **IX**: Dark Annealing of PERC cells at 300 °C (left) and 175 °C (right) monitored by open circuit measurements; no pronounced systematic change is observed throughout the experiment. The symbol colours relate to base wafer doping as defined in Table 1.

cleaved cell edges during dark annealing. This hypothesis is supported by the result of **Experiment VIIb** where the PL proxy method was applied to monitor dark annealing of a full solar cell (see crossed symbols in Fig. 4a)). While the systematic PL signal increase was still observed, it was less pronounced and thus more in line with the voltage measurements in **Experiment VIII**.

Samples that underwent dark annealing at 300 °C (**Experiment IX**) did not exhibit pronounced changes, as shown in the left part of Fig. 4b). Performing such dark annealing prior to other tests also did not cause different subsequent reaction to LeTID testing, as demonstrated by the half-filled symbols in Figs. 3 and 4. This is in contrast to the observations of Grant et al. for earlier Ga-PERC cell batches from the same manufacturer [16,17].

4. Discussion

Our experiments did not indicate a significant impact of the Ga doping concentration on the behaviour of the samples. We observed the expected impact of doping on lifetime levels (see e.g. Fig. 2) and slightly different solar cell parameters – but that was expected due to effects such as Auger recombination and series resistance. The studied doping concentration range was *insufficiently large* to rule out the existence of a gallium concentration influence but *large enough* that strong effects – such as a direct linear impact on degradation kinetics or magnitude – should have been revealed. The observed degradation-recovery cycles observed upon testing samples with strong bulk hydrogenation (see Fig. 1) confirmed earlier indications that Ga-doped Cz silicon *is* susceptible to LeTID. Thus, the shift from boron doping to gallium doping did not by itself mitigate the issue, as it did for LID caused by the BO-defect [14,15]. In agreement with numerous observations on boron-doped materials, we observed degradation in the strongly hydrogenated lifetime samples while samples without dedicated hydrogen introduction – were more stable (see Appendix Fig. 1).

We observe characteristic LeTID behaviour of samples doped with either boron or gallium with significant degradation both in accelerated tests and under simulated module operation conditions, as shown in Fig. 1. This finding supports the suggestion of Maischner et al. that accelerated LeTID testing conditions of 2 sun equivalent and 140 °C are capable of detecting instability [28]. Interestingly, we did not observe an onset of surface passivation degradation on the Cz-Si:Ga samples in our experimental timeframe, although parallel experiments with boron-doped material show effects. Fig. 1 shows lifetime curves for boron-doped samples for comparison (crossed orange data points). In the Cz-Si:B material the effects of BO-LID and LeTID overlap and cause a drastic lifetime degradation, which complicates a qualified discussion [41] but the FZ-Si:B samples clearly show pronounced surface recombination increase after the bulk degradation has finished – in good agreement with the findings of Sperber et al. [10].

We did not observe typical LeTID defect activation during dark annealing in Cz-Si:Ga. If present it should be noticeable in Fig. 2 (**Experiment III**) for highly hydrogenated lifetime samples or in Fig. 4 (**Experiments VII** & **VIII**) for finished PERC cells. This is in contrast to findings by Chen et al. on boron-doped multicrystalline and Cz-Si [35] and on boron-doped FZ silicon by e.g. Hammann et al. [30]. This may imply that defect activation in the dark is not possible in Cz-Si:Ga wafers. Kwapil et al. did report degradation of a hydrogen-rich Cz-Si:Ga sample upon dark annealing at 175 °C of unknown origin [18]. As discussed in section 3.1 we confirmed that the degradation observed by Kwapil et al. and that in **Experiment III** are likely related to recombination in the wafer bulk. The fact that our curve fitting interpreted the degradation as a J_{0s} increase aligns well with a recent discussion by Herguth et al. who pointed out that under certain conditions surface and bulk recombination behave similarly [32]. Given that the degradation under illumination (**Experiments I** & **II**) was clearly different in terms of injection dependent recombination and showed similarities to SRD reported by Sperber et al. [10], it seems this degradation during dark annealing is not the activation of LeTID defects. While the exact mechanisms for LeTID and SRD are still under debate, there appears to be consensus on the involvement of hydrogen [2–4,7,9–11]. The behaviour of hydrogen in boron-doped silicon has been investigated in several recent studies [30,42–46] and studies with Cz-Si:Ga have found that the higher stability of GaH pairs compared to BH pairs has a strong impact on hydrogen distribution [38,47]. Our results are well in line with findings of somewhat different extent and kinetics of LeTID when compared to B-doped material by e.g., Kwapil et al. [18] or Winter et al. [7]. The acceptor species does not need to be directly involved in the LeTID defect to have a strong impact on degradation stability.

In earlier studies, we demonstrated that a 30 min dark anneal at 300 °C changed the LeTID testing response of Ga-PERC cells similar to those investigated in this work [16,17]. The cells tested in this current work originate from a more recent batch of cell production – and we can report they now exhibit the same stable behaviour with and without this additional dark anneal.

The biggest changes we observed on PERC cells in this study occurred upon dark annealing at 175 °C (see Fig. 4a)) – signal changes of up to 35 % PL intensity were observed, implying ~5 mV potential voltage change. A comparable improvement in V_{oc} was also observed on a PERC cell after the 300 °C pre-annealing (half-filled green triangles in Fig. 4b)). However, this specific cell started well below the level of the other cells and so the improvement is rather a recovery to the expected level. It may have been caused by passivation of surface flaws or microcracks at the elevated temperature. Since all observed significant changes were actual small *improvements,* we do not regard them reason for concern on cell performance stability.

5. Conclusion

Our experiments on lifetime samples (**Experiments I-III**) confirm that LeTID can in fact occur in Cz-Si:Ga wafers. The degradation was less pronounced than in B-doped samples processed and tested alongside this study and appears to be delayed but it could still affect the in-field performance of PERC cells. The degradation was found under low and high illumination intensity at 75 °C and also during the accelerated LeTID test of 2 sun eq. illumination at 140 °C suggested by Maischner et al. [28]. We did not observe surface related degradation [10] on Cz-Si:Ga samples in any of our illuminated experiments. This may indicate that the effect is suppressed or at least delayed by Ga-doping, which may be related to the higher stability of GaH pairs compared to BH pairs. Dark annealing of the Cz-Si:Ga samples did not give rise to activation of LeTID defects in contrast to observations on B-doped material [30,35] and earlier reports on a Cz-Si:Ga wafer [18]. Interestingly however, we did observe a pronounced increase of surface recombination (in terms of J_{0s}) after ~200 h.

Our experiments performed on solar cells (**Experiments IV-IX**) indicate that, in practice, LeTID does not affect industrial PERC cell production of at least one major supplier. We tested PERC cells under several conditions resembling different operation conditions and the accelerated LeTID test but found no relevant degradation. This includes the cells to be stable after 300 °C dark annealing, which led to LeTID susceptibility in earlier product generations [16,17]. A significant increase of PL intensity was observed during dark annealing experiments, but further studies indicated this increase did not translate to relevant changes of the cell parameters and was instead likely related to sample preparation (i.e., passivation of local flaws such as cleaved edges).

Several recent studies have investigated the impact of LeTID on Ga-PERC and/or means to reduce or suppress it, e.g., Refs. [7,17,20,28,34,48]. While no details on the specific production process of the investigated PERC solar cells can be disclosed here, it can be stated that a suitable combination of dielectric passivation layers and thermal treatments – especially for metal contact formation – with Cz-Si:Ga effectively suppresses LeTID. As Cz-Si:Ga is not affected by light-induced degradation due to BO-Defects [15], it allows for different optimisation paths especially concerning bulk hydrogenation.

CRediT authorship contribution statement

T. Niewelt: Writing – review & editing, Writing – original draft, Visualization, Resources, Methodology, Investigation, Formal analysis, Data curation, Conceptualization. **F. Maischner:** Writing – review & editing, Investigation, Data curation. **W. Kwapil:** Writing – review & editing, Supervision, Project administration, Methodology, Funding acquisition, Conceptualization. **E. Khorani:** Writing – review & editing, Investigation. **S.L. Pain:** Writing – review & editing, Investigation. **Y. Jung:** Writing – review & editing, Investigation. **E.C.B. Hopkins:** Investigation. **M. Frosch:** Investigation. **P.P. Altermatt:** Writing – review & editing, Resources. **H. Guo:** Writing – review & editing, Resources. **Y.C. Wang:** Writing – review & editing, Resources. **N.E. Grant:** Writing – review & editing, Resources, Methodology, Investigation, Conceptualization. **J.D. Murphy:** Writing – review & editing, Supervision, Resources, Project administration, Funding acquisition, Conceptualization.

Declaration of competing interest

The authors declare the following financial interests/personal relationships which may be considered as potential competing interests: H.G. and Y.C.W. are employed by LONGi Green Energy Technology Co. and P.P.A. is employed by Trina Solar Limited. The authors acknowledge that both companies may have a commercial interest in this study. The corresponding author (T.N.) hereby confirms that these interests did not influence the reported outcomes of the study.

Data availability

Data underpinning figures in this paper can be freely downloaded from https://wrap.warwick.ac.uk/181279/. Requests for additional data should be made directly to the corresponding author.

Acknowledgement

This work was supported by the Leverhulme Trust (RPG-2020-377), the Engineering and Physical Sciences Research Council (EPSRC) Charged Oxide Inversion Layer (COIL) solar cells project (EP/V037749/1), and by the German Federal Ministry for Economic Affairs and Climate Action under contract numbers 03EE1133A, 03EE1133B, 03EE1052B and 03EE1052D. S.L.P. acknowledges funding from the EPSRC Doctoral Training Partnership (EP/R513374/1). The authors would like to acknowledge Bernd Steinhauser for providing analysis software for lifetime measurement batch processing, Benjamin Hammann for fruitful discussions on hydrogen complexes, and the reviewers for detailed and insightful comments.

Appendix. Supplementary data

Material quality & stability with low hydrogenation

As mentioned in the contribution, we also prepared samples with intentionally low bulk hydrogenation. This set of lifetime samples (*lowH*) served to demonstrate the lifetime potential of the material and whether any instabilities would occur even in hydrogen-lean process schemes. Samples from ~1 Ωcm wafers (Material A) were coated with 25 nm per side of different layers using plasma-enhanced ALD. Some samples were coated with Al_2O_3 using an Oxford Instruments OpAL tool at Fraunhofer ISE and the passivation was subsequently activated by annealing at 425 °C in forming gas. Other samples were coated using a Veeco Fiji ALD system at University of Warwick with either Al_2O_3 or HfO_2 at a deposition temperature of 200 °C with a remote O_2 plasma co-reactant and subsequently activated by annealing at 460 °C in air (as discussed in Ref. [49]). The ALD-passivated samples did not undergo a diffusion gettering step.

Charge carrier lifetime measurements were performed on these less hydrogenated samples. The samples featured effective lifetimes exceeding 1 ms at 10^{15} cm^{-3} injection despite the small sample size and individual handling during sample preparation. Measurements after several days of storage in the dark did not reveal significant changes in the measured lifetime (not shown). This implies negligible impacts of potential iron contamination even without a gettering step, c.f, [19,50]. The lifetime results hence demonstrate that the investigated Cz-Si:Ga of Material A to be of good crystallographic quality and purity, which is likely transferrable for the other tested materials. When the samples were subject to LeTID testing under the same conditions as **Experiment I** (~0.15 sun eq. illumination at 75 °C), the effective lifetime of the samples was found to be very stable over time, as shown in Appendix Fig. 1a).

To assess surface passivation quality and get an idea of its stability, we evaluated all measured effective lifetime curves by fitting the surface recombination parameter J_{0s}. The used lifetime measurement and J_{0s} fitting routine for evaluation were not optimized for taking impacts of bulk lifetime on J_{0s} into account (c.f., [31,32]). This likely contributes to variations of J_{0s} with overall lifetime level and the reported J_{0s} should be regarded rather as qualitative tracking of changes rather than precise values. The surface passivation quality achieved with the ALD processes was found to be very good and robust against the low intensity testing conditions, as shown in Appendix Fig. 1b), where extracted single-side J_{0s} are shown.

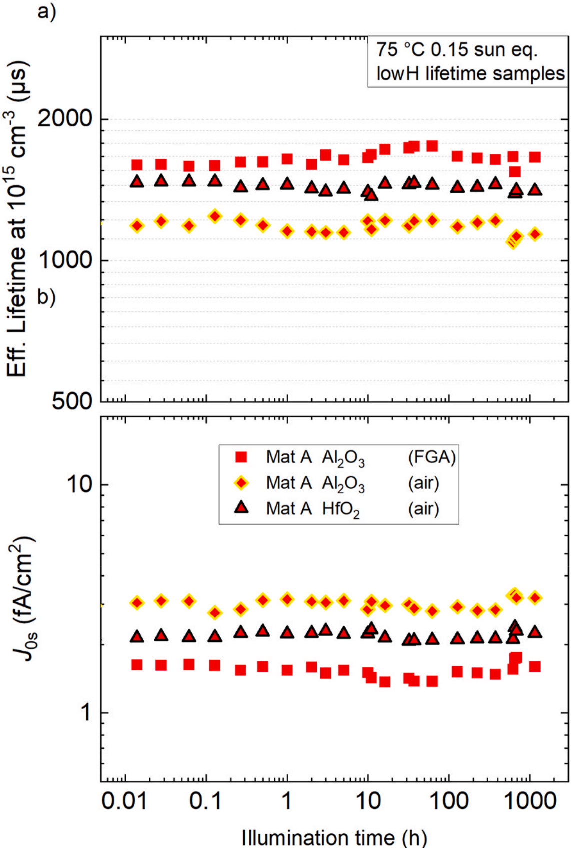

Appendix Fig. 1. Measurement results of LeTID testing on *lowH* lifetime samples (ALD Al_2O_3 and HfO_2 surface passivation) under low intensity LeTID testing, i.e., **Experiment I.** a): Effective charge carrier lifetimes τ_{eff} extracted at $\Delta n = 10^{15}$ cm^{-3}. b): Fitted surface recombination parameter J_{0s}.

Sample resistivity tracking

The dark sheet resistance of the samples measured by WCT-120 before flashing was monitored in search of conductivity changes that would imply significant formation or dissolution of acceptor-hydrogen complexes, as discussed e.g. by Walter et al. [29] or Hammann et al. [30]. We observed sheet resistance changes during dark annealing (**Experiment III**, see Fig. 2) but they are rather small. Sample conductivity is very sensitive to temperature variation and the used WCT-120 setups feature a rather rudimentary temperature control. Thus, fluctuations in laboratory temperature or oscillations related to slow chuck temperature control may introduce unwanted variations across time series such as the ones in this study. Therefore Appendix Fig. 2 shows the recorded sheet resistance values of our other time series experiments for reference. Besides demonstrating that **Experiment III** recorded a distinctly different behaviour this data set may serve as comparison for similar studies.

Appendix Fig. 2a shows sheet resistance measurements on three samples from Cz-Si:Ga Material A. The two samples annealed in air originated from the same wafer, while the third sample was cut from a sister wafer. An inter-sample variation in sheet resistance level of ~2 Ω/□ is observed. This likely arises from small variations of wafer thickness and lateral doping concentration across the host wafers. There may also be small effects caused by the differing amount of negative fixed charge between the different dielectric layers. The measured sheet resistance of the three samples is found to exhibit jumps and gradual changes by ~1 Ω/□ but stay rather stable overall. If we assume the samples with low bulk hydrogenation should not undergo significant changes during low intensity LeTID testing in bulk resistivity this variation gives an impression of the measurement uncertainty/ error in our study.

A similar amount of fluctuations was observed for the strongly hydrogenated Cz-Si:Ga and Cz-Si:B samples low intensity LeTID testing (Experiment I) and the accelerated LeTID test (**Experiment II**), as shown in Appendix Fig. 2b) and c).

Interestingly, slight changes were observed in the two FZ-Si:B samples during the first few hours of low intensity testing (see Appendix Fig. 2b)). This may hint towards reactions involving BH pairs, but a more detailed analysis was beyond the scope of this work.

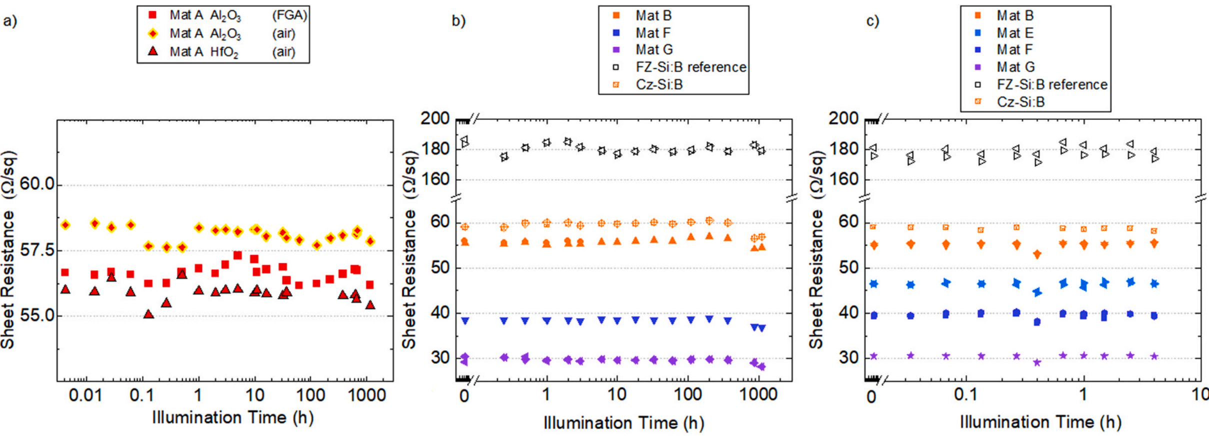

Appendix Fig. 2. Sheet resistance of lifetime samples during LeTID different tests. a) low intensity LeTID testing of lowly hydrogenated samples of Material A. b) low intensity LeTID testing of strongly hydrogenated lifetime samples (**Experiment I**). c) Accelerated LeTID testing of hydrogenated lifetime samples (**Experiment II**).

Appendix. PL proxy method

Within reasonable assumptions for the used solar cells and observed PL intensity changes, the relative change of PL intensity compared to initial intensity I_{PL0} relates to a change of open circuit device voltage $\Delta V_{oc} \approx \frac{k_B T}{q} \ln \frac{I_{PL}}{I_{PL0}}$ with q being the elementary charge, T the temperature in Kelvin and the Boltzmann constant k_B. A precise consideration would need to take the impact of band gap narrowing on radiative recombination into account [51, 52], which is beyond the scope and requirements of the study presented here.

References

[1] K.Z. Ramspeck, S, H. Nagel, A. Metz, Y. Gassenbauer, B. Birkmann, A. Seidl, Light induced degradation of rear passivated mc-Si solar cells, in: 27th European Photovoltaic Solar Energy Conference and Exhibition, 2012, pp. 861–865, https://doi.org/10.4229/27thEUPVSEC2012-2DO.3.4.

[2] D. Chen, P.G. Hamer, M. Kim, T.H. Fung, G. Bourret-Sicotte, S. Liu, C.E. Chan, A. Ciesla, R. Chen, M.D. Abbott, B.J. Hallam, S.R. Wenham, Hydrogen induced degradation: a possible mechanism for light- and elevated temperature- induced degradation in n-type silicon, Sol. Energy Mater. Sol. Cell. 185 (2018) 174–182, https://doi.org/10.1016/j.solmat.2018.05.034.

[3] D. Chen, M. Vaqueiro Contreras, A. Ciesla, P. Hamer, B. Hallam, M. Abbott, C. Chan, Progress in the understanding of light- and elevated temperature-induced degradation in silicon solar cells: a review, Prog. Photovoltaics Res. Appl. 29 (2020) 1180–1201, https://doi.org/10.1002/pip.3362.

[4] T. Niewelt, F. Schindler, W. Kwapil, R. Eberle, J. Schön, M.C. Schubert, Understanding the light-induced degradation at elevated temperatures: similarities between multicrystalline and floatzone p-type silicon, Prog. Photovoltaics Res. Appl. 26 (2018) 533–542, https://doi.org/10.1002/pip.2954.

[5] T. Niewelt, M. Selinger, N.E. Grant, W. Kwapil, J.D. Murphy, M.C. Schubert, Light-induced activation and deactivation of bulk defects in boron-doped float-zone silicon, J. Appl. Phys. 121 (2017), 185702, https://doi.org/10.1063/1.4983024.

[6] H.C. Sio, H. Wang, Q. Wang, C. Sun, W. Chen, H. Jin, D. Macdonald, Light and elevated temperature induced degradation in p-type and n-type cast-grown multicrystalline and mono-like silicon, Sol. Energy Mater. Sol. Cell. 182 (2018) 98–104, https://doi.org/10.1016/j.solmat.2018.03.002.

[7] M. Winter, D. Walter, J. Schmidt, Carrier lifetime degradation and regeneration in gallium- and boron-doped monocrystalline silicon materials, IEEE J. Photovoltaics 11 (2021) 866–872, https://doi.org/10.1109/jphotov.2021.3070474.

[8] F. Kersten, F. Fertig, K. Petter, B. Klöter, E. Herzog, M.B. Strobel, J. Heitmann, J. W. Müller, System performance loss due to LeTID, Energy Proc. 124 (2017) 540–546, https://doi.org/10.1016/j.egypro.2017.09.260.

[9] D. Bredemeier, D.C. Walter, R. Heller, J. Schmidt, Impact of hydrogen-rich silicon nitride material properties on light-induced lifetime degradation in multicrystalline silicon, Phys. Status Solidi Rapid Res. Lett. 13 (2019), 1900201, https://doi.org/10.1002/pssr.201900201.

[10] D. Sperber, A. Heilemann, A. Herguth, G. Hahn, Temperature and light-induced changes in bulk and passivation quality of boron-doped float-zone silicon coated with SiNx:H, IEEE J. Photovoltaics 7 (2017) 463–470, https://doi.org/10.1109/jphotov.2017.2649601.

[11] D. Sperber, A. Herguth, G. Hahn, A 3-state defect model for light-induced degradation in boron-doped float-zone silicon, Phys. Status Solidi Rapid Res. Lett. 11 (2017), 1600408, https://doi.org/10.1002/pssr.201600408.

[12] H. Kodera, Diffusion coefficients of impurities in silicon melt, Jpn. J. Appl. Phys. 2 (1963) 212–219, https://doi.org/10.1143/jjap.2.212.

[13] T. Hoshikawa, X. Huang, S. Uda, T. Taishi, Segregation of Ga during growth of Si single crystal, J. Cryst. Growth 290 (2006) 338–340, https://doi.org/10.1016/j.jcrysgro.2006.01.026.

[14] S.W. Glunz, S. Rein, J. Knobloch, W. Wettling, T. Abe, Comparison of boron- and gallium-doped p-type Czochralski silicon for photovoltaic application, Prog. Photovoltaics Res. Appl. 7 (1999) 463–469, https://doi.org/10.1002/(sici)1099-159x(199911/12)7:6<463::Aid-pip293>3.0.Co;2-h.

[15] T. Niewelt, J. Schön, W. Warta, S.W. Glunz, M.C. Schubert, Degradation of crystalline silicon due to boron–oxygen defects, IEEE J. Photovoltaics 7 (2016) 383–398, https://doi.org/10.1109/JPHOTOV.2016.2614119.

[16] N.E. Grant, J.R. Scowcroft, A.I. Pointon, M. Al-Amin, P.P. Altermatt, J.D. Murphy, Lifetime instabilities in gallium doped monocrystalline PERC silicon solar cells, Sol. Energy Mater. Sol. Cell. 206 (2020), 110299, https://doi.org/10.1016/j.solmat.2019.110299.

[17] N.E. Grant, P.P. Altermatt, T. Niewelt, R. Post, W. Kwapil, M.C. Schubert, J. D. Murphy, Gallium-doped silicon for high-efficiency commercial passivated emitter and rear solar cells, Sol. RRL 5 (2021), 2000754, https://doi.org/10.1002/solr.202000754.

[18] W. Kwapil, J. Dalke, R. Post, T. Niewelt, Influence of dopant elements on degradation phenomena in B-and Ga-doped Czochralski-grown silicon, Sol. RRL 5 (2021), 2100147, https://doi.org/10.1002/solr.202100147.

[19] R. Post, T. Niewelt, W. Kwapil, M.C. Schubert, Carrier lifetime limitation of industrial Ga-doped Cz-grown silicon after different solar cell process flows, IEEE J. Photovoltaics 12 (2021) 238–243, https://doi.org/10.1109/JPHOTOV.2021.3116017.

[20] M. Winter, D.C. Walter, J. Schmidt, Impact of fast-firing conditions on light- and elevated-temperature-induced degradation (LeTID) in Ga-doped Cz-Si, IEEE J. Photovoltaics 13 (2023) 849–857, https://doi.org/10.1109/JPHOTOV.2023.3304118.

[21] S. Jafari, M. Figg, Z. Hameiri, Investigation of light-induced degradation in gallium- and indium-doped Czochralski silicon, Sol. Energy Mater. Sol. Cell. 251 (2023) 112121, https://doi.org/10.1016/j.solmat.2022.112121.

[22] C. Chen, H. Yang, J. Wang, J. Lv, H. Wang, Investigating the viability of PERC solar cells fabricated on Ga- instead of B-doped monocrystalline silicon wafer, Sol. Energy Mater. Sol. Cell. 227 (2021) 111134, https://doi.org/10.1016/j.solmat.2021.111134.

[23] B. Vicari Stefani, M. Kim, M. Wright, A. Soeriyadi, D. Andronikov, I. Nyapshaev, S. Abolmasov, K. Emtsev, A. Abramov, B. Hallam, Stability study of silicon heterojunction solar cells fabricated with gallium- and boron-doped silicon wafers, Sol. RRL 5 (2021) 2100406, https://doi.org/10.1002/solr.202100406.

[24] Y. Zhi, J. Zheng, M. Liao, W. Wang, Z. Liu, D. Ma, M. Feng, L. Lu, S. Yuan, Y. Wan, B. Yan, Y. Wang, H. Chen, M. Yao, Y. Zeng, J. Ye, Ga-doped Czochralski silicon with rear p-type polysilicon passivating contact for high-efficiency p-type solar cells, Sol. Energy Mater. Sol. Cell. 230 (2021) 111229, https://doi.org/10.1016/j.solmat.2021.111229.

[25] M. Winter, D.C. Walter, B. Min, R. Peibst, R. Brendel, J. Schmidt, Light and elevated temperature induced degradation and recovery of gallium-doped Czochralski-silicon solar cells, Sci. Rep. 12 (2022) 8089, https://doi.org/10.1038/s41598-022-11831-3.

[26] S. Jafari, M. Abbott, D. Zhang, J. Wu, F. Jiang, Z. Hameiri, Bulk defect characterization in metalized solar cells using temperature-dependent Suns-Voc

measurements, Sol. Energy Mater. Sol. Cell. 236 (2022) 111530, https://doi.org/10.1016/j.solmat.2021.111530.

[27] F. Maischner, S. Maus, J. Greulich, S. Lohmüller, E. Lohmüller, P. Saint-Cast, D. Ourinson, H. Vahlman, K. Hergert, S. Riepe, S. Glunz, S. Rein, LeTID mitigation via an adapted firing process in p-type PERC cells from SMART cast-monocrystalline, Czochralski and high-performance multicrystalline silicon, Prog. Photovoltaics Res. Appl. 30 (2021) 123–131, https://doi.org/10.1002/pip.3467.

[28] F. Maischner, W. Kwapil, J.M. Greulich, Y. Jung, H. Höffler, P. Saint-Cast, M. C. Schubert, S. Rein, S.W. Glunz, Process influences on LeTID in Ga-doped silicon, Sol. Energy Mater. Sol. Cell. 260 (2023) 112451, https://doi.org/10.1016/j.solmat.2023.112451.

[29] D.C. Walter, D. Bredemeier, R. Falster, V.V. Voronkov, J. Schmidt, Easy-to-apply methodology to measure the hydrogen concentration in boron-doped crystalline silicon, Sol. Energy Mater. Sol. Cell. 200 (2019) 109970, https://doi.org/10.1016/j.solmat.2019.109970.

[30] B. Hammann, L. Rachdi, W. Kwapil, F. Schindler, M.C. Schubert, Insights into the hydrogen-related mechanism behind defect formation during light- and elevated-temperature-induced degradation, Phys. Status Solidi Rapid Res. Lett. 15 (2021), 2000584, https://doi.org/10.1002/pssr.202000584.

[31] B. Hammann, B. Steinhauser, A. Fell, R. Post, T. Niewelt, W. Kwapil, A. Wolf, A. Richter, H. Höffler, M.C. Schubert, Quantifying surface recombination—improvements in determination and simulation of the surface recombination parameter J_{0s}, IEEE J. Photovoltaics 13 (2023) 535–546, https://doi.org/10.1109/jphotov.2023.3265859.

[32] A. Herguth, J. Kamphues, On the impact of bulk lifetime on the quantification of recombination at the surface of semiconductors, IEEE J. Photovoltaics 13 (2023) 672–681, https://doi.org/10.1109/jphotov.2023.3291453.

[33] D. Sperber, A. Graf, D. Skorka, A. Herguth, G. Hahn, Degradation of surface passivation on crystalline silicon and its impact on light-induced degradation experiments, IEEE J. Photovoltaics 7 (2017) 1627–1634, https://doi.org/10.1109/jphotov.2017.2755072.

[34] F. Maischner, J.M. Greulich, W. Kwapil, D. Ourinson, S.W. Glunz, S. Rein, LeTID mitigation via an adapted firing process in p-type PERC cells from gallium-doped Czochralski silicon, Sol. Energy Mater. Sol. Cell. 262 (2023) 112529, https://doi.org/10.1016/j.solmat.2023.112529.

[35] D. Chen, M. Kim, B.V. Stefani, B.J. Hallam, M.D. Abbott, C.E. Chan, R. Chen, D.N. R. Payne, N. Nampalli, A. Ciesla, T.H. Fung, K. Kim, S.R. Wenham, Evidence of an identical firing-activated carrier-induced defect in monocrystalline and multicrystalline silicon, Sol. Energy Mater. Sol. Cell. 172 (2017) 293–300, https://doi.org/10.1016/j.solmat.2017.08.003.

[36] A. Herguth, On the meaning(fullness) of the intensity unit 'suns' in light induced degradation experiments, Energy Proc. 124 (2017) 53–59, https://doi.org/10.1016/j.egypro.2017.09.339.

[37] R. Post, T. Niewelt, W. Yang, D. Macdonald, W. Kwapil, M.C. Schubert, Re-evaluation of the SRH-parameters for the FeGa defect, in: AIP Conference Proceedings, 2147, 2019, 020012, https://doi.org/10.1063/1.5123817.

[38] J. Simon, A. Herguth, L. Kutschera, G. Hahn, The dissociation of gallium–hydrogen pairs in crystalline silicon during illuminated annealing, Phys. Status Solidi Rapid Res. Lett. 16 (2022), 2200297, https://doi.org/10.1002/pssr.202200297.

[39] N.E. Grant, T. Niewelt, N.R. Wilson, E.C. Wheeler-Jones, J. Bullock, M. Al-Amin, M. C. Schubert, A.C. van Veen, A. Javey, J.D. Murphy, Superacid-treated silicon surfaces: extending the limit of carrier lifetime for photovoltaic applications, IEEE J. Photovoltaics 7 (2017) 1574–1583, https://doi.org/10.1109/JPHOTOV.2017.2751511.

[40] J.D. Murphy, N.E. Grant, S.L. Pain, T. Niewelt, A. Wratten, E. Khorani, V. P. Markevich, A.R. Peaker, P.P. Altermatt, J.S. Lord, Carrier lifetimes in high-lifetime silicon wafers and solar cells measured by photoexcited muon spin spectroscopy, J. Appl. Phys. 132 (2022), 065704, https://doi.org/10.1063/5.0099492.

[41] A. Herguth, On the lifetime-equivalent defect density: properties, application, and pitfalls, IEEE J. Photovoltaics 9 (2019) 1182–1194, https://doi.org/10.1109/jphotov.2019.2922470.

[42] B. Hammann, N. Assmann, P.M. Weiser, W. Kwapil, T. Niewelt, F. Schindler, R. Sondena, E.V. Monakhov, M.C. Schubert, The impact of different hydrogen configurations on light- and elevated-temperature- induced degradation, IEEE J. Photovoltaics 13 (2023) 224–235, https://doi.org/10.1109/jphotov.2023.3236185.

[43] D.C. Walter, V.V. Voronkov, R. Falster, D. Bredemeier, J. Schmidt, On the kinetics of the exchange of hydrogen between hydrogen–boron pairs and hydrogen dimers in crystalline silicon, J. Appl. Phys. 131 (2022), 165702, https://doi.org/10.1063/5.0086307.

[44] J. Simon, A. Herguth, G. Hahn, Quantitative analysis of boron–hydrogen pair dynamics by infrared absorption measurements at room temperature, J. Appl. Phys. 131 (2022), 235703, https://doi.org/10.1063/5.0090965.

[45] V.V. Voronkov, Independent subsystems of atomic hydrogen in silicon responsible for boron passivation and for dimer production, Phys. Status Solidi A 219 (2022), 2200081, https://doi.org/10.1002/pssa.202200081.

[46] P. Hamer, B. Hallam, R.S. Bonilla, P.P. Altermatt, P. Wilshaw, S. Wenham, Modelling of hydrogen transport in silicon solar cell structures under equilibrium conditions, J. Appl. Phys. 123 (2018), 043108, https://doi.org/10.1063/1.5016854.

[47] Y. Acker, J. Simon, A. Herguth, Formation dynamics of BH and GaH-pairs in crystalline silicon during dark annealing, Phys. Status Solidi A 219 (2022), 2200142, https://doi.org/10.1002/pssa.202200142.

[48] J. Simon, R. Fischer-Süßlin, R. Zerfaß, P. Dufke, L. Kutschera, A. Herguth, S. Roder, G. Hahn, Correlation study between LeTID defect density, hydrogen and firing profile in Ga-doped crystalline silicon, solar energy materials and solar cells, Sol. Energy Mater. Sol. Cells 260 (2023) 112456, https://doi.org/10.1016/j.solmat.2023.112456.

[49] A. Wratten, S.L. Pain, D. Walker, A.B. Renz, E. Khorani, T. Niewelt, N.E. Grant, J. D. Murphy, Mechanisms of silicon surface passivation by negatively charged hafnium oxide thin films, IEEE J. Photovoltaics 13 (2023) 40–47, https://doi.org/10.1109/jphotov.2022.3227624.

[50] R. Basnet, C. Sun, T. Le, Z. Yang, A. Liu, Q. Jin, Y. Wang, D. Macdonald, Investigating wafer quality in industrial Czochralski-grown gallium-doped p-type silicon ingots with melt recharging, Sol. RRL 7 (2023) 2300304, https://doi.org/10.1002/solr.202300304.

[51] P.P. Altermatt, F. Geelhaar, T. Trupke, X. Dai, A. Neisser, E. Daub, Injection dependence of spontaneous radiative recombination in crystalline silicon: experimental verification and theoretical analysis, Appl. Phys. Lett. 88 (2006), 261901, https://doi.org/10.1063/1.2218041.

[52] A. Fell, T. Niewelt, B. Steinhauser, F.D. Heinz, M.C. Schubert, S.W. Glunz, Radiative recombination in silicon photovoltaics: modeling the influence of charge carrier densities and photon recycling, Sol. Energy Mater. Sol. Cell. 230 (2021), 111198, https://doi.org/10.1016/j.solmat.2021.111198.